Kinetic and Nuclear Magnetic Resonance Study of the Interaction of $NADP^+$ and NADPH with Chicken Liver Fatty Acid Synthase†

Gary F. Leanz and Gordon G. Hammes*

Department of Chemistry, Cornell University, Ithaca, New York 14853-1301

Received March 17, 1986; Revised Manuscript Received May 13, 1986

ABSTRACT: The ionic strength dependence of the second-order rate constant for the association of reduced nicotinamide adenine dinucleotide phosphate (NADPH) and chicken liver fatty acid synthase was determined. This rate constant is 7.2×10^7 M^{-1} s^{-1} at zero ionic strength and 25 °C; the effective charge at the cofactor binding sites is +0.8. The conformations of nicotinamide adenine dinucleotide phosphate ($NADP^+$) and NADPH bound to the β-ketoacyl and enoyl reductase sites were determined from transferred nuclear Overhauser effect measurements. Covalent modification of the enzyme with pyridoxal 5′-phosphate abolished cofactor binding at the enoyl reductase site; this permitted the cofactor conformations at the β-ketoacyl and enoyl reductase sites to be distinguished. For $NADP^+$ bound to the enzyme, the conformation of the nicotinamide–ribose bond is anti at the enoyl reductase site and syn at the β-ketoacyl reductase site; the adenine–ribose bond is anti, and the sugar puckers are C3′-endo. Nicotinamide–adenine base stacking was not detected. Structural models of $NADP^+$ at the β-ketoacyl and enoyl reductase sites were constructed by using the distances calculated from the observed nuclear Overhauser effects. Because of the overlap of the resonances of several nonaromatic NADPH protons with the resonances of HDO and ribose protons, less extensive structural information was obtained for NADPH bound to the enzyme. However, the conformations of NADPH bound to the two reductases are qualitatively the same as those of $NADP^+$, except that the nicotinamide moiety of NADPH is closer to being fully anti at the enoyl reductase site.

Chicken liver fatty acid synthase is a multifunctional enzyme that catalyzes the synthesis of long-chain fatty acids according to the overall reaction

$$\text{acetyl-CoA} + n\,\text{malonyl-CoA} + 2n\,\text{NADPH} + 2n\,H^+ \rightarrow CH_3(CH_2CH_2)_nCOOH + (n+1)\text{CoA} + 2n\,NADP^+ + (n-1)H_2O + nCO_2 \quad (1)$$

Fatty acid synthases have been reviewed extensively (Volpe & Vagelos, 1973; Bloch & Vance, 1977; Wakil et al., 1983; Hammes, 1985). Among the seven partial reactions catalyzed by the mammalian enzyme are two NADPH[1]-dependent reductions: the reduction of a carbonyl group (β-ketoacyl reductase) and the reduction of a carbon–carbon double bond (enoyl reductase) of the growing fatty acyl chain. Chicken liver fatty acid synthase is a dimer of two identical polypeptide chains of molecular weight 250000 (Hsu & Yun, 1970), each of which contains one β-ketoacyl reductase and one enoyl reductase site (Wakil et al., 1983).

In this work, the effective charge at the NADPH binding sites was determined from a Debye–Hückel analysis of the ionic strength dependence of the second-order rate constant for the association of NADPH with the enzyme. The conformations of $NADP^+$ and NADPH bound to the enzyme were determined from ^1H–^1H intramolecular transferred nuclear Overhauser effects. The interactions of $NADP^+$ (or NADPH) with the two different reductases are characterized by identical binding constants, but cofactor binding at the enoyl reductase site was selectively and quantitatively blocked by covalent modification of the enzyme with pyridoxal 5′-phosphate, thereby permitting separate analyses of the β-ketoacyl and enoyl reductase sites.

Materials and Methods

Chemicals. NADPH, $NADP^+$, dithiothreitol, pyridoxal 5′-phosphate, $NaBH_4$, and CoA esters were from Sigma. *N*-Acetyl-*S*-(acetoacetyl)cysteamine was from Research Specialties. D_2O, 99.8 atom % D, was from Aldrich; D_2O, 100% D, low in paramagnetic impurities, was from Stohler. All other chemicals were high-quality commercial grades, and all solutions were prepared with deionized water.

Enzyme. Chicken liver fatty acid synthase was prepared and assayed according to Cognet and Hammes (1985). The specific activity of the enzyme was greater than 1.6 units/mg. The enzyme was modified with pyridoxal 5′-phosphate as described by Poulose & Kolattukudy (1980), except that 10 μM enzyme was treated once with 4 mM pyridoxal 5′-phosphate at 30 °C for 15 min in a shallow, silanized beaker and then reduced on ice with 10 mM $NaBH_4$ (omitting octanol). For small-scale experiments, unreacted small molecules and degradation products were removed by passage through a Sephadex G-25 centrifuge column (Neal & Florini, 1973). For NMR experiments, the reaction mixture was transferred to an Amicon Centricon-30 microconcentrator, which removed unused reactants and degradation products by ultrafiltration. β-Ketoacyl reductase activity was assayed as the decrease in NADPH absorbance due to reduction of *N*-acetyl-*S*-(acetoacetyl)cysteamine; this activity was not altered by modification of the enzyme with pyridoxal 5′-phosphate. Enoyl reductase activity, assayed as the decrease in NADPH absorbance due to reduction of crotonyl-CoA, was not detected after the pyridoxal phosphate modification. This modified enzyme had 2.0 NADPH binding sites, as determined by fluorescence

† This work was supported by National Institutes of Health Grant GM 13292, National Science Foundation Grant PCM 8120818, and National Science Foundation Instrumentation Program Grant PCM 8018643 to the Cornell Nuclear Magnetic Resonance Facility.

[1] Abbreviations: CoA, coenzyme A; EDTA, ethylenediaminetetraacetic acid; $NADP^+$, nicotinamide adenine dinucleotide phosphate; NADPH, reduced $NADP^+$; NOE, nuclear Overhauser effect.

0006-2960/86/0425-5617$01.50/0

titration (Cardon & Hammes, 1983).

Stopped-Flow Measurements. Kinetic experiments were performed on a modified Durrum-Gibson stopped-flow spectrophotometer (Cognet et al., 1983). The binding of NADPH to the enzyme was studied by mixing NADPH with the enzyme at 25 °C in potassium phosphate of the desired ionic strength at pH 7.0, 0.1 mM EDTA, and observing changes in NADPH fluorescence when it binds to fatty acid synthase (364–367-nm excitation, >420-nm emission; Dugan & Porter, 1971). Because it quenches NADPH fluorescence, dithiothreitol was removed immediately before kinetic experiments by passing enzyme solutions through a Sephadex G-25 centrifuge column. The enzyme concentration was 0.2 μM after mixing in the stopped-flow apparatus, and NADPH concentrations were 3.5–20.0 μM after mixing.

Optical Measurements. Absorbance measurements were performed on a Varian/Cary 2200 spectrophotometer, and fluorescence was measured on a Perkin-Elmer MPF-44B fluorimeter. The extinction coefficients (ϵ) at the wavelengths (subscripts, nm) of the concentration determinations were as follows: fatty acid synthase, $\epsilon_{279} = 4.82 \times 10^5$ M^{-1} cm^{-1}, M_r = 500 000 (Hsu & Yun, 1970); NADPH, $\epsilon_{340} = 6220$ M^{-1} cm^{-1} (Horecker & Kornberg, 1948); crotonyl-CoA, $\epsilon_{266} =$ 22 600 M^{-1} cm^{-1} (Stadtman, 1957); other CoA esters, $\epsilon_{260} =$ 14 600 M^{-1} cm^{-1} (Dugan & Porter, 1970).

NMR Spectroscopy. Cofactors were dissolved in phosphate buffer and lyophilized twice from D_2O in the dark. pD equals the pH as measured with a glass electrode plus 0.4 (Glasoe and Long, 1960). Lyophilization destroyed enzyme activity; therefore, for NMR experiments, the enzyme was deuterated and concentrated to 40–100 mg/mL in Amicon Centricon-30 microconcentrators at room temperature. Ultrafiltration was carried out with repeated washes of 0.1 M phosphate buffer in 98% D_2O (pD 7.2) with a final wash of buffer made from 99.996% D_2O; NMR samples ultimately contained 98–99 atom % D. Fatty acid synthase and β-ketoacyl reductase activities were assayed before and after NMR experiments, and these specific activities declined no more than 15 % in any 24-h experiment. To avoid denaturation of the enzyme, solutions were not degassed; however, dissolved oxygen has a negligible effect on the spin–lattice relaxation time of protons bound to large molecules, where the cross-relaxation rates are fast. Enzyme concentrations were typically 0.2 mM (0.8 mM in NADPH binding sites). Coenzyme solutions in buffered D_2O were added gradually, and spectra were examined to find the lowest free to bound coenzyme ratio with averaged signals that were sufficiently narrow; this ratio was generally 5–15.

^1H NMR spectra were measured with a Varian XL-400 spectrometer at 400 MHz using a 32-bit digitizer, 3200 data points, a spectral width of 4000 Hz, and a filter bandwidth of 2200 Hz. Samples of 0.25–0.5 mL were placed in 5-mm glass NMR tubes and spun at 15 s^{-1}; no more than 2% of the protein precipitated after 24 h. All NMR experiments were conducted at 20 °C. Chemical shifts (δ) are expressed relative to sodium 2,2-dimethyl-2-silapentane-5-sulfonate; residual HDO served as an internal reference (δ 4.800).

The pulse sequence used for the transferred NOE measurements was $[(t_{NOE}-\pi/2-t_{acq}-t_{del})_{32}]_n$, where t_{NOE} was the time (0.05–0.8 s) of NOE buildup by selective irradiation at a chosen frequency, the $\pi/2$ pulse was 13–19 ms, t_{acq} was the acquisition time (0.4 s), and t_{del} was a 3-s delay to allow complete recovery of magnetization of all protons to their equilibrium values prior to perturbation by the selective radiofrequency field. Repetitive cycling through free induction decays corresponding to different decoupling frequencies (a set of 32 scans preceded by four dummy scans) suppressed degradation from long-term instabilities. The irradiation power used (18–24 DB below 0.2 W) was sufficient to be in the high-power limit so that saturation could effectively be considered instantaneous, but with selectivity, so that only a single averaged resonance at a time was saturated (Dobson et al., 1982). Optimum decoupling power varied for different enzyme concentrations and free to bound ratios of ligand. Saturation of the free nucleotide resonances was complete for $t_{NOE} \geq 50$ ms. Blocks of 32 scans at each frequency were accumulated, and the sequence was repeated until 576–1024 scans were obtained. Free induction decays were subtracted from a control irradiated at 1.8 ppm (away from ligand resonances but within the protein manifold to minimize nonspecific NOEs). To minimize truncation effects from the acquisition time of 0.4 s, 2-Hz exponential line broadening was applied prior to Fourier transformation. NOEs are expressed as the decimal fraction of the integral of an irradiated resonance compared to the control. In the presence of enzyme, all transferred NOEs from bound ligand are negative, since $\omega\tau_c \gg 1$, where ω is the Larmor frequency and τ_c the correlation time of the complex.

Data Processing. Best fits of the data to the ionic strength and NMR equations were obtained by the nonlinear least-squares algorithm of Marquardt (1963; Bevington, 1969).

Table I: Kinetic Parameters for the Interaction of NADPH with Fatty Acid Synthase at Various Ionic Strengths[a]

μ (mM)	k_f (μM^{-1} s^{-1})	k_r (s^{-1})	K_D (μM)
7.01	43.6	46.1	1.06
12.0	53.9	49.8	0.92
16.0	40.9	68.3	1.67
27.0	29.7	69.1	2.25
138	20.9	71.0	3.41
227	12.7	76.7	6.00

[a] 25 °C, ≤1 mM EDTA, and various concentrations of potassium phosphate, pH 7.0.

RESULTS

Rate of NADPH Binding to Enzyme. The kinetics of NADPH binding to enzyme are consistent with the mechanism (Cognet et al., 1983)

$$E + NADPH \underset{k_r}{\overset{k_f}{\rightleftharpoons}} E{\cdot}NADPH \qquad (2)$$

The observed pseudo-first order rate constant near equilibrium is

$$k_{obsd} = k_f([NADPH]_e + n[E]_e) + k_r \qquad (3)$$

where n is the number of equivalent NADPH binding sites on the enzyme (4 for native enzyme), and the subscript e denotes equilibrium concentrations. The method of successive approximations used to determine the values of k_f and k_r has been described by Cognet et al. (1983). The rate constants determined at various ionic strengths (μ) are summarized in Table I. Ionic strengths were calculated with the assumption that KH_2PO_4 dissociates completely and K_2HPO_4 dissociates according to the equilibrium $[KHPO_4^-]/([K^+][HPO_4^{2-}]) =$ 4.0 M^{-1} (Smith & Alberty, 1956). Both k_f and k_r varied with ionic strength, but the association rate constant, k_f, contributed most of the ionic strength dependence of the equilibrium dissociation constant, K_D.

Figure 1 shows the dependence of k_f on ionic strength; these data were analyzed with the relationship (cf. Hammes, 1978)

$$\log k_f = \log k_f^0 + 1.02Z_E Z_N \mu^{1/2}/(1 + B\mu^{1/2}) \qquad (4)$$

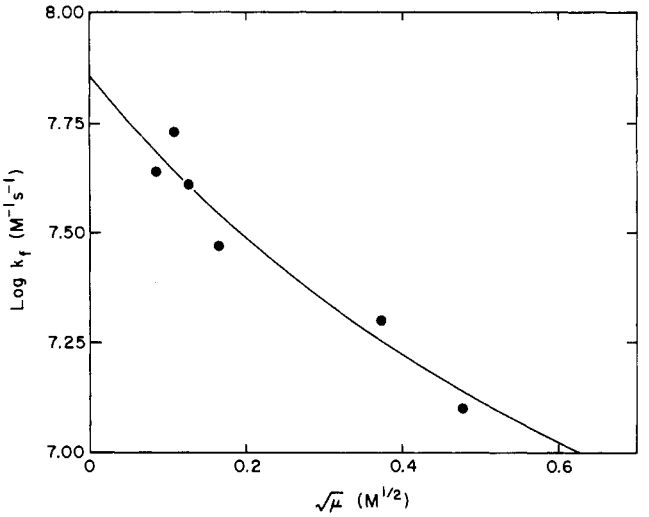

FIGURE 1: Dependence of the bimolecular rate constant (k_f) for the binding of NADPH to fatty acid synthase on the square root of ionic strength ($\mu^{1/2}$). Stopped-flow experiments were carried out at 25 °C in various concentrations of potassium phosphate, pH 7.0 and ≤1 mM EDTA. The line is the best fit to eq 4.

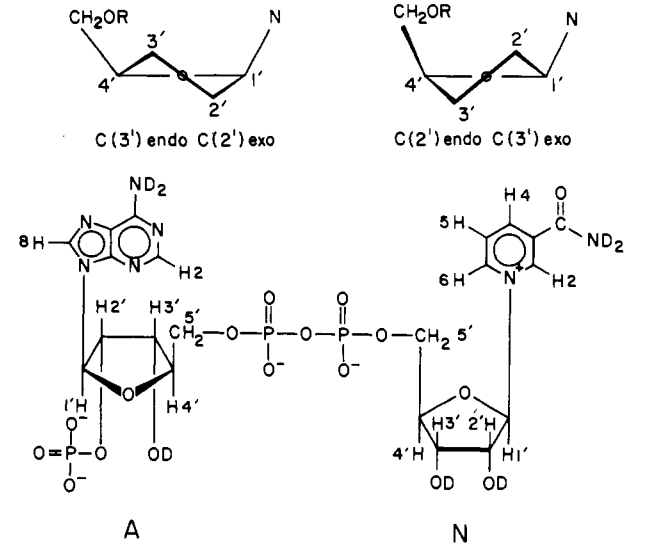

FIGURE 2: Numbering system for the protons of NADP+ drawn with adenine (A) in the anti conformation and nicotinamide (N) in the syn conformation. Sugar pucker nomenclature is also shown.

where μ is the ionic strength, k_f^0 is the association rate constant when $\mu = 0$, Z_E is the effective charge of the binding sites, and Z_N is the effective charge of NADPH. In this study, pH = 7.0 and $Z_N = -3.8$ (Wijnands et al., 1984). Nonlinear least-squares analysis of the data in Figure 1 according to eq 4 gave $k_f^0 = (7.21 \pm 0.37) \times 10^7$ M^{-1} s^{-1}, $Z_E = +0.82 \pm 0.16$, and $B = 1.00 \pm 0.15$. The curve in Figure 1 was calculated with these parameters and eq 4.

NMR of Enzyme-Bound NADP+ and NADPH. The NMR spectrum of NADP+ in the presence of enzyme showed broadened lines, but the chemical shifts of the peaks changed by no more than 5 Hz compared to those of free NADP+. The numbering of protons in NADP+ is indicated in Figure 2, which is drawn with adenine in the syn conformation and nicotinamide in the anti conformation. A typical NMR spectrum of NADP+ with enzyme present is shown in Figure 4A; Figure 6A shows the analogous spectrum for NADPH.

The conformations of nicotinamide cofactors bound to the enzyme were studied by measurement of the transferred nuclear Overhauser effect (Clore & Gronenborn, 1982, 1983). This analysis is valid only for conformationally rigid molecules

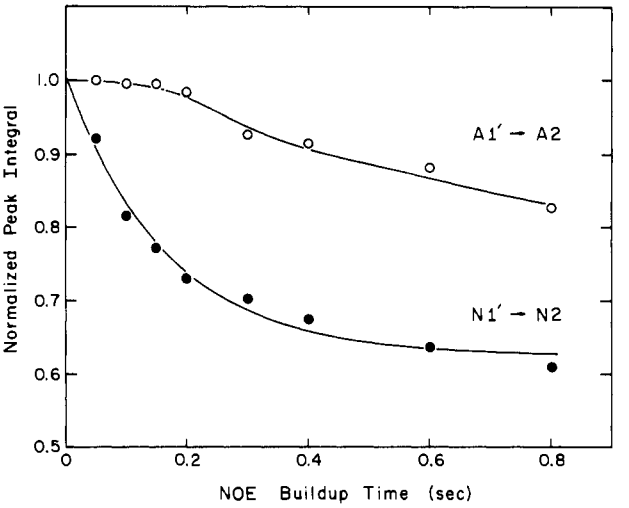

FIGURE 3: Time dependence of transferred nuclear Overhauser effects observed for the averaged H_{A2} and H_{N2} resonances of 5.3 mM NADP+ in the presence of 0.12 mM fatty acid synthase in 0.1 M potassium phosphate, pD 7.4 (99% D) at 20 °C. Indirect cross-relaxation via spin diffusion (A1′–A2) and direct two-spin cross-relaxation (N1′–N2) are illustrated.

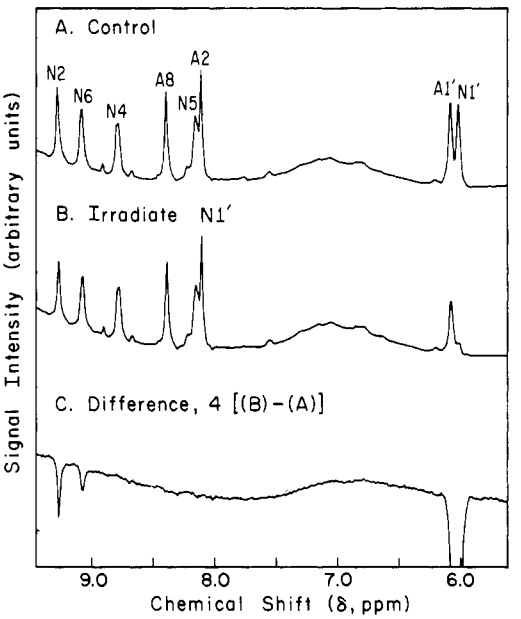

FIGURE 4: Transferred nuclear Overhauser effects in NADP+ bound to fatty acid synthase. The solution contained 5.3 mM NADP+ and 0.12 mM fatty acid synthase in 0.1 M potassium phosphate, pD 7.4 (99% D) at 20 °C. The following spectra are shown: (A) control of NADP+ plus enzyme; (B) irradiation of the averaged N1′ resonance for 0.4 s; (C) difference spectrum [(B) − (A)] enlarged 4-fold. A total of 576 transients was accumulated for each spectrum. Peak assignments are from Oppenheimer (1982).

(Jardetzky & Roberts, 1981). In this work, it was assumed that the enzyme fixes the conformation of the ligand at each site. For an NOE measurement, a specific proton of the bound nucleotide is irradiated; cross-relaxation of this irradiated proton with other nearby protons can occur. Cofactors bound to large macromolecules, because of their long correlation times, generate NMR peaks that are too broad for direct study. When chemical exchange occurs fast enough, however, magnetization can be transferred to free cofactor, and the resultant changes in the intensities of these narrow peaks can be easily measured (Noggle & Schirmer, 1971).

Structural information on the conformation of a bound ligand can be obtained from transferred NOE measurements since the cross-relaxation rate σ_{ij} is proportional to $(r_{ij})^{-6}$, where

Table II: Transferred NOEs for the Nicotinamide Moiety of $NADP^+$ and NADPH Bound to Fatty Acid Synthase[a]

		NOE (%)					
		$NADP^+$			NADPH		
irrad resonance	obsd resonance	native enzyme	β-ketoacyl reductase[b]	enoyl reductase[c]	native enzyme	β-ketoacyl reductase[b]	enoyl reductase[c]
$H_{N1'}$	H_{N2}	−24	−16	−32	*d*	*d*	*d*
$H_{N2'/3'}$	H_{N2}	−12	−10	−14	−12	−8	−16
$H_{N4'}$	H_{N2}	−7	−4	−11			
$H_{N5'(R)}$	H_{N2}	−7	−5	−9	−13[e]	−9[e]	−17[e]
$H_{N5'(S)}$	H_{N2}	−12	−19	−5			
$H_{N1'}$	H_{N6}	−10	−14	−6	*d*	*d*	*d*
$H_{N2'/3'}$	H_{N6}	−14	−8	−20	−26	−12	−38
$H_{H4'}$	H_{N6}	−8	0	−16			
$H_{N5'(R)}$	H_{N6}	−8	−9	−7	−18[e]	−3[e]	−33[e]
$H_{N5'(S)}$	H_{N6}	−13	−12	−14			
H_{N5}	H_{N6}	−20	−23	−17	*d*	*d*	*d*
H_{N6}	H_{N5}	−21	−20	−22	*f*	*f*	*f*
H_{N4}	H_{N5}	−21	−20	−22	*f*	*f*	*f*
H_{N5}	H_{N4}	−19	−18	−20	*d*	*d*	*d*

[a] 0.1 M potassium phosphate, pD 7.4, 20 °C. Unprimed numbers refer to protons on the nicotinamide ring; primed numbers denote protons on the adjacent ribose. [b] From NOE measurements of cofactors bound to pyridoxal 5′-phosphate modified enzyme. [c] Calculated from eq 6. [d] Not measurable because the irradiated N1′ resonance (δ 4.789) overlaps with the solvent HDO resonance (δ 4.800). [e] Sum of the NOEs generated by the three irradiated resonances shown at left. [f] Not measurable because the observed N5 resonance (δ 4.784) overlaps with the solvent HDO resonance.

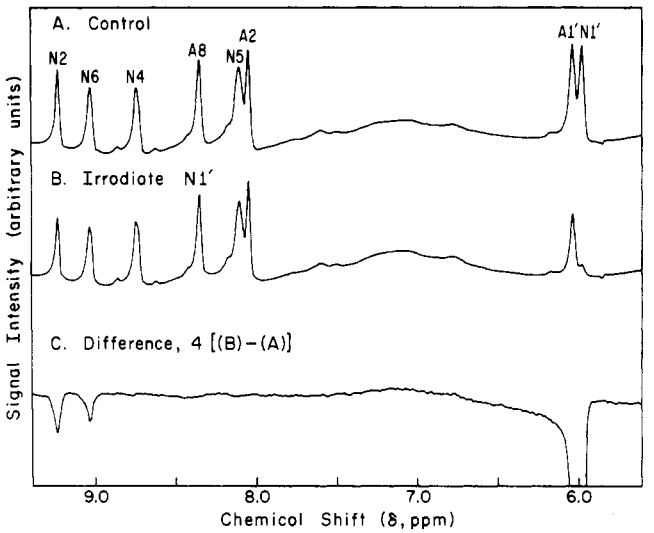

FIGURE 5: Transferred nuclear Overhauser effects for $NADP^+$ bound to fatty acid synthase modified with pyridoxal 5′-phosphate. The solution contained 10.9 mM $NADP^+$ and 0.14 mM modified enzyme in 0.1 M potassium phosphate, pD 7.4 (99% D) at 20 °C. The following spectra are shown: (A) control of $NADP^+$ plus enzyme; (B) irradiation of the averaged N1′ resonance for 0.4 s; (C) difference spectrum [(B)−(A)] enlarged 4-fold. A total of 640 transients was accumulated for each spectrum. Peak assignments are from Oppenheimer (1982).

r_{ij} is the distance between bound ligand protons i and j. Thus, distance ratios can be obtained from the relationship

$$r_{ij}/r_{kl} = (\sigma_{kl}/\sigma_{ij})^{1/6} \cong [N_{kl}(t)/N_{ij}(t)]^{1/6} \qquad (5)$$

if the correlation times of the two interproton vectors i–j and k–l are the same. Here $N_{kl}(t)$ and $N_{ij}(t)$ are the measured NOEs at time t between the subscripted protons. Some typical spectra demonstrating NOEs for $NADP^+$ binding to native enzyme and pyridoxal 5′-phosphate modified enzyme are shown in Figures 4 and 5. Analogous spectra for NADPH binding to the same enzyme species are shown in Figures 6 and 7. Tables II and III summarize the NOEs for all measurable pairs of protons of $NADP^+$ and NADPH when bound to the enzyme and to pyridoxal 5′-phosphate modified enzyme. The NMR data from native enzyme arise from equal binding of cofactors to the β-ketoacyl and enoyl reductase sites, whereas NMR data from modified enzyme result solely from cofactor binding to the β-ketoacyl reductase sites. The NOEs

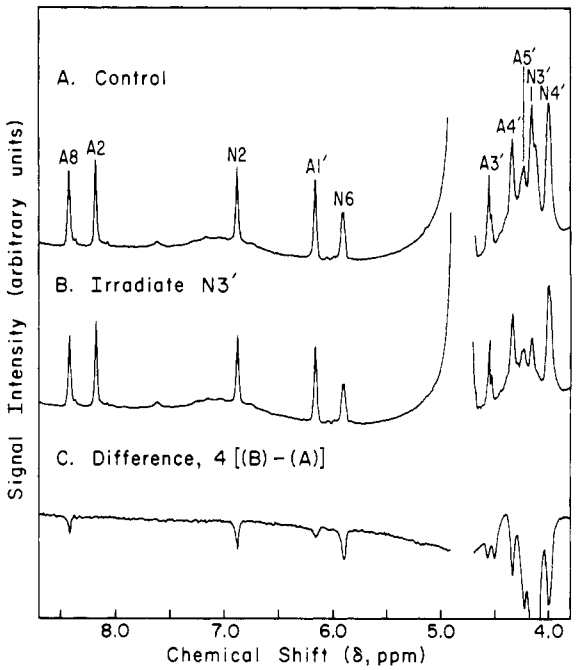

FIGURE 6: Transferred nuclear Overhauser effects for NADPH bound to fatty acid synthase. The solution contained 9.8 mM NADPH and 0.13 mM fatty acid synthase in 0.1 M potassium phosphate, pD 7.4 (99% D) at 20 °C. The following spectra are shown: (A) control of NADPH plus enzyme; (B) irradiation of the averaged N3′ resonance for 0.4 s; (C) difference spectrum [(B) − (A)] enlarged 4-fold. A total of 448 transients was accumulated for each spectrum. Peak assignments are from Oppenheimer (1982).

due to $NADP^+$ or NADPH bound to the enoyl reductase site were calculated with the assumption that an NOE from the native enzyme is the average of the NOEs from the two types of reductase sites:

$$NOE_{native} = (NOE_{enoyl} + NOE_{\beta\text{-ketoacyl}})/2 \qquad (6)$$

The average can be used in this case because the equilibrium dissociation constants for the binding of cofactors to the two different reductases are identical, and the NOEs are normalized. Distances were calculated from eq 5 for all pairs showing NOE >3% with an irradiation time of 0.4 s, and the results are presented in Tables IV and V.

The observed NOE arising from irradiation of either the averaged resonance of free and bound ligand or the resonance

Table III: Transferred NOEs for the Adenine Moiety of NADP$^+$ and NADPH Bound to Fatty Acid Synthase[a]

		NOE (%)					
		NADP$^+$			NADPH		
irrad resonance	obsd resonance	native enzyme	β-ketoacyl reductase[b]	enoyl reductase[c]	native enzyme	β-ketoacyl reductase[b]	enoyl reductase[c]
$H_{A1'}$	H_{A8}	−5	−6	−4	−5	−5	−5
$H_{A2'}$	H_{A8}	−18	−21	−15	−17	−20	−14
$H_{A3'}$	H_{A8}	−11	−9	−13	−6	−9	−3
$H_{A4'}$	H_{A8}	−9	−3	−15	−5	−6	−4
$H_{A5'(R)}$	H_{A8}	−1	−3	0	−3	0	−6
$H_{A5'(S)}$	H_{A8}	−9	−6	−12	−5	−2	−8
$H_{A1'}$	H_{A2}	−2	0	−4	0	0	0
$H_{A2'}$	H_{A2}	−1	0	−2	0	0	0
$H_{A3'}$	H_{A2}	−1	0	−2	−1	−1	−1
$H_{A4'}$	H_{A2}	−3	0	−6	−2	0	−4
$H_{A5'(R)}$	H_{A2}	−2	0	−4	0	0	0
$H_{A5'(S)}$	H_{A2}	0	−1	0	0	0	0
H_{N6}	H_{A2}	0	0	0	0	0	0
H_{A2}	H_{N6}	−2	0	−4	−2	0	−4
H_{N2}	H_{A2}	−1	0	−2	0	0	0
H_{A2}	H_{N2}	0	0	0	−2	−2	−2

[a] 0.1 M potassium phosphate, pD 7.4, 20 °C. [b] From NOE measurements of cofactors bound to pyridoxal 5′-phosphate modified enzyme. [c] Calculated from eq 6.

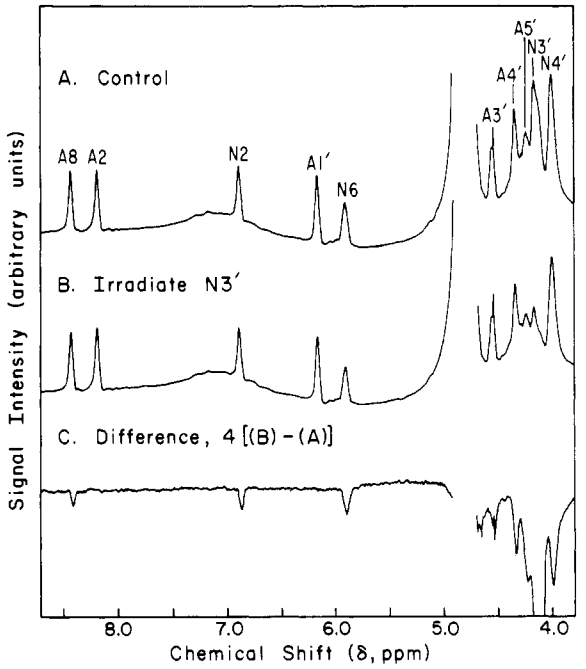

FIGURE 7: Transferred nuclear Overhauser effects for NADPH bound to fatty acid synthase modified with pyridoxal 5′-phosphate. The solution contained 7.9 mM NADPH and 0.11 mM modified enzyme in 0.1 M potassium phosphate, pD 7.4 (99% D) at 20 °C. The following spectra are shown: (A) control of NADPH plus enzyme; (B) irradiation of the averaged N3′ resonance for 0.4 s; (C) difference spectrum [(B) − (A)] enlarged 4-fold. A total of 384 transients was accumulated for each spectrum. Peak assignments are from Oppenheimer (1982).

of free ligand (in the case of fast exchange on the cross-relaxation scale) is given by (Clore & Gronenboron, 1983)

$$(d(NOE)/dt)_{t=0} = -(P_b\sigma_B + P_f\sigma_F) \quad (7)$$

where σ_B and σ_F are the cross-relaxation rates for bound and free molecules and P_b and P_f are the fractions of bound and free ligands, respectively. In all cases, transferred NOEs were maximal after irradiation at positions corresponding to free ligand resonances, indicating that chemical exchange between bound and free NADP$^+$ and NADPH was fast on the chemical shift scale. For irradiation times ≤0.5 s, the NOEs observed for free nucleotide were positive and < 0.03, so that the observed NOEs depended primarily on σ_B. The observed NOEs were small because of the low sample concentrations (mM) and the lack of degassing of the solutions.

Table IV: Cross-Relaxation Rates and Distances between Protons of NADP$^+$ Bound to the β-Keotacyl and Enoyl Reductases of Fatty Acid Synthase

NADP$^+$ proton pair	β-ketoacyl reductase[a]		enoyl reductase[b]	
	σ_B[c] (s^{-1})	r[d] (Å)	σ_B[c] (s^{-1})	r[d] (Å)
N5–N6	4.6	2.48[e]	4.6	2.48[e]
N4–N5	4.4	2.5	4.8	2.5
N1′–N2	3.5	2.6	7.0	2.3
N2′,3′–N2	2.2	2.8	3.1	2.7
N5′(*R*)–N2	1.1	3.2	2.0	2.9
N5′(*S*)–N2	4.2	2.5	1.1	3.2
N1′–N6	3.1	2.7	2.6	2.7
N2′,3′–N6	1.8	2.9	4.4	2.5
N5′(*R*)–N6	2.0	2.9	1.5	3.0
N5′(*S*)–N6	2.6	2.7	3.1	2.7
A2′–A8	4.6	2.5	3.3	2.6
A3′–A8	2.0	2.9	2.8	2.7
A5′(*S*)–A8	1.1	3.2	3.3	2.6

[a] Calculated from the NOE data for pyridoxal 5′-phosphate modified enzyme. [b] Calculated from the difference of the NOE data for native enzyme and those for the β-ketoacyl reductase by use of eq 6. [c] Cross-relaxation rates between protons were calculated (eq 5) from the ratios of the observed NOEs, using the value of the initial slope of the NOE buildup curve for N5–N6 as the standard. [d] Calculated from eq 5 with the assumption that r(N5–N6) = 2.48Å. [e] Assumed from standard bond lengths and angles.

Figure 3 shows the development of NOEs for two typical resonances as a function of the selective irradiation time. A lag in NOE buildup such as the effect on A2 after irradiation of A1′ is due to spin diffusion (Clore & Gronenborn, 1983), presumably through nearby protons of the enzyme. A smooth exponential NOE buildup curve (e.g., Figure 3, N1′ → N2) established the authenticity of each of the observed NOEs. The cross-relaxation rates of the control (N5–N6) protons were calculated from the initial slope of the NOE buildup curves. However, for the overall analysis of bond lengths and angles, eq 5 was used since Clore & Gronenborn (1985) have established the superiority of measuring NOEs at one well-chosen time point that maximizes the NOE and minimizes spin diffusion.

For NADP$^+$, the data for the adenine–ribose glycosidic bond are unambiguous: A2 is not close to any ribose protons in any experiment, showing that the conformation is anti at both the

Table V: Cross-Relaxation Rates and Distances between Protons of NADPH Bound to the β-Ketoacyl and Enoyl Reductases of Fatty Acid Synthase

NADPH proton pair	β-ketoacyl reductase[a]		enoyl reductase[b]	
	σ_B[c] (s^{-1})	r[d] (Å)	σ_B[c] (s^{-1})	r[d] (Å)
N5–N6	4.6	2.48[e]	4.6	2.48[e]
N2′,3′–N2	1.8	2.9	4.8	2.5
N2′,3′–N6	2.6	2.7	8.8	2.2
A2′–A8	4.4	2.5	3.1	2.7
A3′–A8	2.0	2.9	1.7	2.9

[a] Calculated from the NOE data for pyridoxal 5′-phosphate modified enzyme. [b] Calculated from the difference of the NOE data for native enzyme and those for the β-ketoacyl reductase by use of eq 6. [c] Cross-relaxation rates between protons were calculated (eq 5) from the ratios of the observed NOEs, using the value of the initial slope of the NOE buildup curve for N5–N6 as the standard. [d] Calculated from eq 5 with the assumption that r(N5–N6) = 2.48 Å. [e] Assumed from standard bond lengths and angles.

β-ketoacyl and enoyl reductase sites. At the β-ketoacyl reductase site (Table IV), A8 is much closer to A2′ than to A3′ (and far from A5′), while at the enoyl reductase site A8 is almost equidistant from A2′ and A3′ (i.e., over the center of the ribose ring) and, as expected, much closer to A5′. Model building gave glycosidic bond angles that differed only slightly: $\chi_A = 150 \pm 20°$ at the β-ketoacyl reductase site and $\chi_A = 180 \pm 20°$ at the enoyl reductase site. For nucleotides, χ, the torsion angle about the C1′–N bond, specifies the orientation of the base relative to the ribose; χ is defined as the solid angle created by the three bonds O4′–C1′–N1–C2 for the nicotinamide moiety (χ_N) and by the three bonds O4′–C1′–N9–C4 for the adenine moiety (χ_A). Rotation of the base relative to the sugar is somewhat restricted sterically (Haschemeyer & Rich, 1967), and two conformational states are preferred: syn ($\chi \sim 0°$) and anti ($\chi \sim 180°$). For the nicotinamide–ribose bond, the interproton distances show that at the β-ketoacyl reductase sites N1′ is closer to N6 than to N2 and N3′ is closer to N2 than to N6; i.e., the nicotinamide–ribose glycosidic bond angle is in the syn range: $\chi_N = 20 \pm 40°$. By contrast, at the enoyl reductase sites, N1′ is much closer to N2 than to N6, and N3′ is closer to N6 than to N2; i.e. the nicotinamide–ribose glycosidic bond angle is in the anti range: $\chi_N = 180 \pm 30°$. The sugar pucker fits a C3′-endo to O1′-endo conformation and a gauche–gauche or trans–gauche conformation at C4′–C5′. No NOEs between any of the nicotinamide ring protons and the adenine protons were seen; therefore, no conclusion could be drawn concerning the relative orientation of these two aromatic rings (Jardetzky & Roberts, 1981).

For NADPH, the data for the adenine–ribose glycosidic bond angle are again straightforward (Table III): A2 is not close to any ribose protons, and the adenine–ribose conformation is, therefore, anti at both the β-ketoacyl and enoyl reductase sites. At the β-ketoacyl reductase site, A8 is again much closer to A2′ than to A3′, and at the enoyl reductase site, A8 is almost equidistant from A2′ and A3′ over the center of the ribose ring (Table V). The best fits for the adenine–ribose glycosidic bond angles were as follows: $\chi_A = 0 \pm 20°$ at the β-ketoacyl reductase site; $\chi_A = 30 \pm 20°$ at the enoyl reductase site. Structural analysis of the nicotinamide moiety was complicated by the loss of aromaticity on reduction of $NADP^+$ to NADPH, thereby moving the chemical shifts of the nicotinamide ring upfield, out of the aromatic region and into crowded regions of the NMR spectrum. Another unfortunate feature of NMR work with NADPH is that one of the most reliable ribose resonances, N1′ (δ 4.789), overlaps with the peak of solvent HDO (δ 4.800) and with that of N5 (δ 4.784). Furthermore, the N4′, N5′(R), and N5′(S) resonances of NADPH overlap, so that only NOEs averaged from all these positions could be recorded. Because of these difficulties, the cross-relaxation rates, interproton distances, and nicotinamide–ribose bond angle of NADPH bound to the enzyme could not be quantified as extensively as for $NADP^+$.

However, the N4′ and N5′ protons lie on the same side of the ribose ring and thus constitute a spatial marker for the side of the ribose ring closer to the diphosphate bridge. NADPH bound at the β-ketoacyl reductase site gave NOEs corresponding to the syn conformation (N2′,3′–N2 and N4′,5′–N6), while NOEs expected for the anti conformation (N2′,3′–N6 and N4′,5′–N2) disappeared when the enoyl reductase site was blocked (Table II), so as for bound $NADP^+$ NADPH at the enoyl reductase site assumed a conformation in the anti range. At the β-ketoacyl reductase sites, N1′ is closer to N6 than to N2, and N3′ is closer to N2 than to N6; the nicotinamide–ribose glycosidic bond angle is in the syn range: $\chi_N = 20 \pm 40°$. At the enoyl reductase sites, N1′ is much closer to N2 than to N6, and N3′ is closer to N6 than to N2; the nicotinamide–ribose glycosidic bond angle is in the anti range: $\chi_N = 180 \pm 30°$. The averaged N2′ and N3′ resonances were superimposed so that no information could be obtained concerning the sugar pucker conformation. No NOEs were observed between adenine and nicotinamide ring protons of NADPH, so that no conclusion could be made about their proximity.

Compared with a control irradiated at −1.5 ppm (outside the protein manifold), no NOEs were observed after irradiation in the methylene region of the protein manifold (δ 1.80). That is, no NOEs between protein and ligand resonances were detected.

Discussion

Extrapolation to zero ionic strength provided an estimate of $k_f° = 7.2 \times 10^7\ M^{-1}\ s^{-1}$ for the association of NADPH with its four binding sites on enzyme. This approaches, but is somewhat less than, the value expected for a diffusion-controlled process (Hammes & Schimmel, 1971). The effective charge of the binding site, +0.8, obtained from the analysis presented here, represents the average charge density at the four NADPH binding sites. The data do not permit the β-ketoacyl and enoyl reductase sites to be distinguished. It would have been most desirable to measure the effective charge at the β-ketoacyl reductase site separately, by studying the ionic strength dependence of NADPH binding to modified enzyme. However, although the β-ketoacyl reductase partial activity remains intact after modification, the dissociation constant for NADPH increases (Cardon & Hammes, 1983), probably due to both the repulsive negative charge of bound pyridoxal 5′-phosphate plus steric hindrance at that site. Furthermore, although four molecules of pyridoxal phosphate per enzyme are involved in actively blocking the enoyl site, a total of 7–20 pyridoxal 5′-phosphate bind per enzyme molecule, depending on the conditions used (Cardon & Hammes, 1983). In this work, about 15 molecules of pyridoxal 5′-phosphate were bound per molecule of modified enzyme. Hence, it would be impossible to interpret an "effective charge number" at modified NADPH binding sites.

Chicken liver fatty acid synthase (M_r 500 000) and bovine liver glutamate dehydrogenase ($M_r \sim 10^6$) (Clore & Gronenborn, 1982) are the two largest enzymes that have been studied with transferred NOE measurements. The normalized magnitude of the transferred NOE increases as the molecular weight of the protein increases (Clore & Gronenborn, 1982),

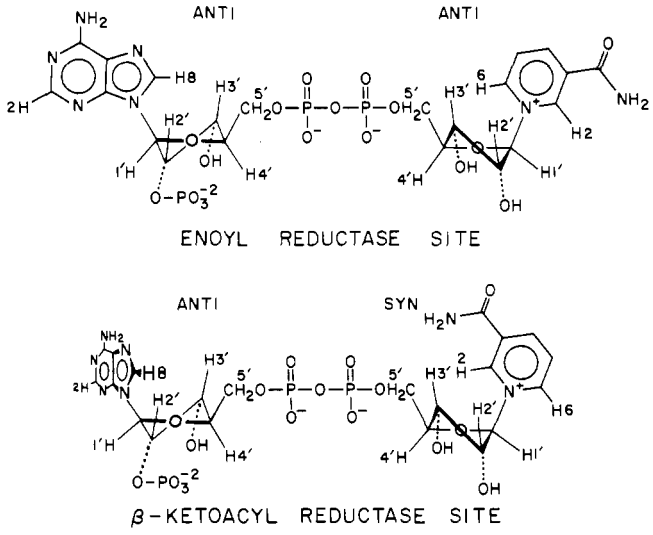

FIGURE 8: Conformations of NADP+ bound to the β-ketoacyl reductase and enoyl reductase sites of fatty acid synthase, as derived from nuclear Overhauser measurements and model building. The orientation of the adenine and nicotinamide rings with respect to each other could not be determined from the data.

so that transferred NOE measurements become especially useful for larger molecular weight systems where X-ray crystallography is increasingly difficult.

Because of uncertainties due to averaging, it is generaly impossible to specify the structure of flexible molecules by NMR: i.e., the "average" structure deduced from the observed NMR parameters may bear no resemblance to the actual chemical structures giving rise to the various signals being averaged (Jardetzky & Roberts, 1981). Hence, in this study, we explicitly assumed that NADP+ or NADPH is bound at each active site in a rigid conformation while NOEs are being built up. This is consistent with the increased NMR line width in the presence of enzyme, compared to that of free ligand. The dissociation rate constant for NADPH indicates that the bound ligands are in fast exchange with free ligands. The dissociation rate constant for NADP+ binding is not known but is probably somewhat larger than for NADPH.

Distance measurements between protons of NADP+ bound to the β-ketoacyl and enoyl reductase sites of the enzyme (Table IV) showed that the conformation of the nicotinamide–ribose bond is anti at the enoyl reductase site and syn at the keto reductase site. The *pro*-4*R* hydrogen of NADPH is transferred to substrate at the enoyl reductase sites of the enzyme, and the *pro*-4*S* hydrogen of NADPH is transferred to substrate at the β-ketoacyl reductase sites (Anderson & Hammes, 1984). Thus, fatty acid synthase conforms with the generalizations obtained both from nuclear Overhauser effects measurements (Levy et al., 1983) and from crystallographic measurements (Moras et al., 1975) that dehydrogenases in which the *pro*-*R* (A-side) hydrogen is transferred bind the nicotinamide ring in the anti conformation; transfer of the *pro*-*S* (B-side) hydrogen correlates with the syn conformation of the nicotinamide–ribose bond. The distance measurements for NADP+ (Table IV) and NADPH (Table V) showed that the adenine–ribose bond is anti in all cases. NOE buildup between A1′ and A8 was characterized by a lag (cf. Figure 3) and therefore represents indirect cross-relaxation via spin diffusion. The anti conformation of the adenine–ribose bond is most typical for nucleotides bound to proteins (Feeney et al., 1979; Levy et al., 1983; Gronenborn et al., 1984a,b).

Transferred NOE measurements showed that the adenine–ribose bond of NADP+ or NADPH bound to isocitrate dehydrogenase is syn (Ehrlich and Colman, 1985), leading to the hypothesis that "enzymes with strong specificity for nucleotides with a 2′-phosphate bind them in a syn conformation". Fatty acid synthase has an absolute requirement for NADPH (with its 2′-phosphate): NADH lacks catalytic activity and binds to the enzyme much more weakly than NADPH. Therefore, the results presented in this paper provide a counterexample to the hypothesis (Ehrlich & Colman, 1985) that preference for nucleotides with a 2′-phosphate favors a syn orientation. In general, a syn conformation correlates with C2′-endo(S) pucker of the ribose ring, especially in the purine series, while χ in the anti range correlates with the C3′-endo(N) sugar pucker (Hruska, 1973). For pyrimidine nucleosides, the anti orientation of the base is finely tuned by the sugar pucker (Altona & Sundaralingam, 1973). However, a large increase in the C3′-endo/anti population occurs when nucleosides are phosphorylated at O5′; in this case, interactions between O5′ and the base are enhanced (Saenger, 1985).

The NOE data in Table III showed that the adenine–ribose bond of NADPH is clearly anti for NADPH (as it is for NADP+) and that little if any change in the orientation of the adenine–ribose bond occurred when the nicotinamide ring was oxidized or reduced. Because the chemical shifts of the nonaromatic nicotinamide protons in NADPH overlap with those of the ribose protons, structural information from transferred NOE studies of NADPH bound to the enzyme was limited. Although the data showed that at both the β-ketoacyl and enoyl reductase sites N2′ and N3′ are closer to N6 than to N2, this geometric result could occur in either a syn or an anti overall conformation, depending on χ_N. No information about the glycosidic bond angle could be deduced from this single NOE measurement.

Crystallographic evidence (Grau, 1982) indicates that binding of NADH or NADPH to many dehydrogenases occurs in an extended form. The lack of transferred NOE between adenine or nicotinamide protons in this study is consistent with an extended binding mode but does not prove that the nicotinamide and adenine rings are farther than 4 Å apart.

The structures of NADP+ at the two reductase sites deduced from NOE distance measurements and molecular models are shown in Figure 8. The relative orientation of the halves of the molecule could not be specified. Although the adenine rings at both sites are anti, NOE measurements revealed different orientations at the two reductase sites. Only a single cofactor structure at each site was assumed, because of the absolute stereospecificity of hydrogen transfer, the large magnitude of the observed NOEs compared to those in solution, and the general requirement of enzymes to align substrates in a highly specific geometry. If this assumption of the rigidity of bound cofactor were false, the NADP+ structures shown would represent a complex average.

Registry No. NADP+, 53-59-8; NADPH, 53-57-6; fatty acid synthase, 9045-77-6; β-ketoacyl reductase, 37250-34-3; enoyl reductase, 37251-09-5.

REFERENCES

Altona, C., & Sundaralingham, M. (1973) *J. Am. Chem. Soc. 95*, 2333–2334.

Anderson, V. A., & Hammes, G. G. (1984) *Biochemistry 23*, 2088–2094.

Bevington, P. R. (1969) *Data Reduction and Error Analysis for the Physical Sciences*, McGraw-Hill, New York.

Bloch, K., & Vance, D. (1977) *Annu. Rev. Biochem. 46*, 263–298.

Cardon, J., & Hammes, G. G. (1983) *J. Biol. Chem. 258*, 4802–4807.

Clore, G. M., & Gronenborn, A. M. (1982) *J. Magn. Reson. 48*, 402–417.
Clore, G. M., & Gronenborn, A. M. (1983) *J. Magn. Reson. 53*, 423–442.
Clore, G. M., & Gronenborn, A. M. (1985) *J. Magn. Reson. 61*, 158–164.
Cognet, J., & Hammes, G. G. (1985) *Biochemistry 24*, 290–297.
Cognet, J., Cox, B. G., & Hammes, G. G. (1983) *Biochemistry 22*, 6281–6287.
Dobson, C. M., Olejniczak, E. T., Poulsen, F. M., & Ratcliffe, R. G. (1982) *J. Magn. Reson. 48*, 87–110.
Dugan, R. E., & Porter, J. W. (1970) *J. Biol. Chem. 245*, 2051–2059.
Dugan, R. E., & Porter, J. W. (1971) *J. Biol. Chem. 246*, 637–642.
Ehrlich, R. S., & Colman, R. F. (1985) *Biochemistry 24*, 5378–5387.
Feeney, J., Batchelor, J. G., Albrand, J. P., & Roberts, G. C. (1979) *J. Magn. Reson. 33*, 519–529.
Glasoe, P. K., & Long, F. A. (1960) *J. Phys. Chem. 64*, 188–191.
Grau, U. M. (1982) in *The Pyridine Nucleotide Coenzymes* (Everse, J., Anderson, B., & You, K.-S., Eds.) pp 135–187, Academic, New York.
Gronenborn, A. M., Clore, G. M., & Jeffery, J. (1984a) *J. Mol. Biol. 172*, 559–572.
Gronenborn, A. M., Clore, G. M., Hobbs, L., & Jeffery, J. (1984b) *Eur. J. Biochem. 145*, 365–371.
Hammes, G. G. (1978) *Principles of Chemical Kinetics*, Academic, New York.
Hammes, G. G. (1985) *Curr. Top. Cell. Regul. 26*, 311–324.
Hammes, G. G., & Schimmel, P. R. (1971) *Enzymes (3rd Ed.) 2*, 67–114.
Haschemeyer, A. E. V., & Rich, A. (1967) *J. Mol. Biol. 27*, 369–384.
Horecker, B. L., & Kornberg, A. (1948) *J. Biol. Chem. 175*, 385–390.
Hruska, F. E. (1973) *Jerusalem Symp. Quant. Chem. Biochem. 5*, 345–360.
Hsu, R. Y., & Yun, S. L. (1970) *Biochemistry 9*, 239–245.
Jardetzky, O., & Roberts, G. C. K. (1981) *NMR in Molecular Biology*, Academic, New York.
Levy, H. R., Ejchart, A., & Levy, G. C. (1983) *Biochemistry 22*, 2792–2796.
Marquardt, D. W. (1963) *J. Soc. Ind. Appl. Math. 11*, 431–441.
Moras, D., Olsen, K. W., Sabesan, M. N., Buchner, M., Ford, G. C., & Rossman, M. G. (1975) *J. Biol. Chem. 235*, 202–204.
Neal, M. W., & Florini, J. R. (1973) *Anal. Biochem. 55*, 328–330.
Noggle, J. H., & Schirmer, R. E. (1971) *The Nuclear Overhauser Effect, Chemical Applications*, Academic, New York.
Oppenheimer, N. J. (1982) in *The Pyridine Nucleotide Coenzymes* (Everse, J., Anderson, B., & You, K.-S., Eds.) pp 51–89, Academic, New York.
Poulose, A. J., & Kolattukudy, P. E. (1980) *Arch. Biochem. Biophys. 201*, 313–321.
Saenger, W. (1985) *Principles of Nucleic Acid Structure*, Springer-Verlag, New York.
Smith, R. M., & Alberty, R. A. (1956) *J. Phys. Chem. 60*, 180–184.
Stadtman, E. R. (1957) *Methods Enzymol. 3*, 931–941.
Volpe, J. J., & Vagelos, P. R. (1973) *Annu. Rev. Biochem. 42*, 21–60.
Wakil, S. J., Stoops, J. K., & Joshi, V. (1983) *Annu. Rev. Biochem. 52*, 539–580.
Wijnands, R. A., van der Zee, J., van Leeuwen, J. W., van Berkel, W. J. H., & Muller, F. (1984) *Eur. J. Biochem. 139*, 637–644.